http://dx.doi.org/10.5012/bkcs.2013.34.5.1366

Phosphorescent Iridium Complexes for OLEDs Based on 1-Phenylpyrazole Ligands with Fluorine and Methyl Moieties

Seung Soo Yoon,* Ji Young Song, Eun Jae Na, Kum Hee Lee, Seong Kyu Kim, Dong Whan Lim,† Seok Jae Lee,† and Young Kwan Kim†,*

*Department of Chemistry, Sungkyunkwan University, Suwon 440-746, Korea. *E-mail: ssyoon@skku.edu*
*†Department of Information Display, Hongik University, Seoul 121-791, Korea. *E-mail: kimyk@hongik.ac.kr*
Received January 18, 2013, Accepted February 6, 2013

A series of phosphorescent iridium(III) complexes **1-4** based on phenylpyrazole were synthesized and their photophysical properties were investigated. To evaluate their electroluminescent properties, OLED devices with the structure of ITO/NPB/mCP: 8% Iridium complexes (**1-4**)/TPBi/Liq/Al were fabricated. Among those, the device with **3** showed the most efficient white emission with maximum luminance of 100.6 cd/m^2 at 15 V, maximum luminous efficiency of 1.52 cd/A, power efficiency of 0.71 lm/W, external quantum efficiency of 0.59%, and CIE coordinates of (0.35, 0.40) at 15.0 V, respectively.

Key Words : Phosphorescence, Iridium complex, Phenylpyrazole ligand, White OLED

Introduction

Phosphorescent organic light emitting diodes (OLEDs) are under intensive investigation because of their potential in improving device performances.[1] Phosphorescent heavy metal complexes play an important role in phosphorescent OLEDs because their strong spin–orbit coupling, caused by the heavy metal atom, makes intersystem crossing between the singlet and triplet excited states more efficient. In theory, mixing the singlet and triplet excited states may lead to internal quantum efficiencies as high as 100%. In particular, cyclometalated iridium(III) complexes show high phosphorescent efficiencies and relatively short lifetimes, and are thus considered as one of the most promising materials for phosphorescent OLEDs.[2-6]

Currently, white OLEDs (WOELDs) receive the intensive focus due to their advantages for large-scale production. Particularly, the single component WOLEDs are the simplest and thus very attractive.[7] For example, using a single emitter, white emission can be generated by combination of blue emission of emitter itself and orange emission from its excimer. Recently, Williams *et al*. reported an efficient WOLED using a phosphorescent complex platinum [2-(4',6'-difluorophenyl)pyridinato-N,C$^{2'}$]](2,4-pentanedionate).[8] Until now, a variety of platinum or iridium complexes as single emitter for efficient WOLEDs have been developed.[9] However, WOLEDs employing single emitter present far-from-ideal electroluminescence (EL) performances for practical applications.

Herein, to use as single emitter for WOLED, phosphorescent iridium(III) complexes (**1-4**), based on 1-phenylpyrazole ligands with fluorine or methyl substitution, were synthesized. Electron donating methyl groups or electron-withdrawing fluorine units were introduced to the phenyl moieties in the phenylpyrazole ligands to tune the band gap of the iridium complexes by controlling the HOMO and LUMO energy levels. As will be seen below, the iridium complexes **1-4** as single emitter with *m*-Bis(*N*-Carbazolyl)-benzene (mCP) host in the emitting layer showed the white emission in OLED devices.

Experimental Section

Synthesis and Characterization. UV-visible absorption spectra were obtained using a Shimadzu UV-1650PC spectrometer. Photoluminescence (PL) spectra were obtained at 77 K using an Aminco-browman series 2 luminescence spectrometer. The HOMO/LUMO energy levels were determined from cyclic voltammetry. The energy band gaps were determined from the inter-section of the absorption and the photoluminescence spectra.

General Procedure for Synthesis of 1: To a flask containing $IrCl_3 \cdot 3H_2O$ (460 mg, 1.54 mmol) and L1 (548 mg, 3.4 mmol) was added a 3:1 mixture of 2-ethoxyethanol and water (12 mL). The mixture was refluxed for 24 h and cooled to room temperature. A colored precipitate was filtered off and washed with water, methanol, and hexane. The crude product was pumped dry to give crude $(L1)_2Ir(\mu\text{-}Cl)_2Ir(L1)_2$. Crude $(L1)_2Ir(\mu\text{-}Cl)_2Ir(L1)_2$ was mixed with Na_2CO_3 (300 mg, 2.7 mmol) in a two-neck flask. 2-ethoxyethanol (10 mL) and 2,4-pentadione (0.14 mL, 1.4 mmol) were added and the mixture was heated at 100 °C for 8 h. The solution was cooled to room temperature and the red solid precipitates were collected by filtration. The orange solid was washed with water, methanol, and hexane. The crude product was purified by column chromatography using 0-40% ethyl acetate in hexane as the eluent. **1** was obtained as solid (410 mg, 44%) after recrystallization from CH_2Cl_2/methanol. ^{1}H-NMR (300 MHz, $CDCl_3$) δ 7.99 (dd, *J* = 1.9 Hz, 0.7 Hz, 2H), 7.57 (dd, *J* = 2.2 Hz, 0.6 Hz, 2H), 7.10 (dd, *J* = 8.6 Hz, 4.7 Hz, 2H), 6.64 (t, *J* = 2.5. 2H), 6.54 (td, *J* = 8.7 Hz, 2.8 Hz, 2H), 5.85 (dd, *J* = 9.2 Hz, 2.6 Hz,

2H), 5.23 (s, 1H), 1.82 (s, 6H); ^{13}C NMR (75 MHz, $CDCl_3$) δ 185.7, 138.1, 126.1, 121.6, 121.3, 111.6, 111.5, 108.5, 108.1, 107.2, 100.6, 28.7; MS(APCI) *m/z*: 614 (M^+); HRMS: [EI^+] calcd. for $C_{23}H_{19}F_2IrN_4O_2$: 614.1105, [M^+]. Found: 614.1097.

Compound 2: (429 mg, 46%) ^{1}H-NMR (300 MHz, $CDCl_3$) δ 8.31 (dd, J = 2.8 Hz, 0.6 Hz, 2H), 7.55 (d, J = 1.9 Hz, 2H), 6.65-6.63 (m, 2H), 6.45-6.37 (m, 2H) 5.63 (dd, J = 8.5 Hz, 2.5 Hz, 2H); ^{13}C NMR (75 MHz, $CDCl_3$) δ 185.8, 138.4, 137.3, 133.4, 133.3, 131.0, 117.1, 116.8 108.5, 107.6, 106.9, 28.7, 28.6; MS (APCI) *m/z*: 650 (M^+); HRMS: [EI^+] calcd. for $C_{23}H_{17}F_4IrN_4O_2$: 650.0917, [M^+]. Found: 650.0908.

Compound 3: (704 mg, 40%). ^{1}H-NMR (300 MHz, $CDCl_3$) δ 8.00 (dd, J = 2.9 Hz, 0.6 Hz, 2H), 7.57 (dd, J = 2.2 Hz, 0.6 Hz, 2H), 7.03 (d, J = 7.9 Hz, 2H), 6.62-6.58 (m, 4H), 6.02 (dd, J = 1.4 Hz, 0.6 Hz, 2H), 5.19 (s, 1H), 2.05 (s, 6H), 1.79 (s, 6H); ^{13}C NMR (75 MHz, $CDCl_3$) δ 185.3, 142.7, 137.6, 136.0, 134.8, 128.4, 125.5, 122.4, 110.4, 106.7, 100.4, 28.7, 21.7; MS (APCI) *m/z*: 606 (M^+); HRMS: [EI^+] calcd. for $C_{25}H_{25}IrN_4O_2$: 606.1607, [M^+]. Found: 606.1601.

Compound 4: (385 mg, 46%). ^{1}H NMR (300 MHz, $CDCl_3$) δ 7.99 (dd, J = 2.8 Hz, 0.6 Hz, 2H), 7.56 (dd, J = 2.1 Hz, 0.7 Hz, 2H), 6.94 (s, 2H), 6.58 (dd, J = 2.7 Hz, 2.3 Hz, 2H), 5.99 (s, 2H), 5.17 (d, 2H), 2.10 (s, 6H), 1.96 (s, 6H), 1.78 (s, 6H); ^{13}C NMR (75 MHz, $CDCl_3$) δ 185.1, 143.1, 137.6, 133.6, 129.3, 125.3, 124.4, 112.1, 106.5, 100.3, 28.7, 20.1, 20.0; MS (APCI) *m/z*: 634; HRMS: [EI^+] calcd. for $C_{27}H_{29}IrN_4O_2$: 634.1920, [M^+]. Found: 634.1916.

Device Fabrication and Measurements. OLEDs using the iridium complex dopants in the emitting layer were fabricated by vacuum (5.0×10^{-7} torr) thermal evaporation onto pre-cleaned ITO coated glass substrates. The general structure was as follows: ITO/NPB (50 nm)/mCP: 8% Ir(III) complexes (30 nm)/TPBi (40 nm)/Alq_3 (20 nm)/Liq (2 nm)/Al. All optical and electrical properties of the devices such as current density, luminance, luminous efficiency and CIE coordinate characteristics were measured with Keithley 236, LS-50B, and MINOLTA CS-100A, respectively.

Results and Discussion

Scheme 1 shows the structures and synthetic routes for the iridium complexes **1-4**. All synthetic procedures were made under nitrogen atmosphere. Ligands **L1-L4** were synthesized according to the procedure described in the literature.[10,11] The iridium complexes were obtained by cyclometalation of the ligands with $IrCl_3$ and subsequent reaction with acetylacetone.

Photophysical data of the iridium complexes **1-4** are given in Table 1. Compared to the low temperature PL spectra of $Ir(ppz)_2acac$, **1** and **2** with fluorine replaced at the 4-position and 2,4-positions of phenyl ring exhibited 12 nm and 36 nm hypochromic shifts, respectively, due to the strong electron-withdrawing ability of fluorine atom. In contrast, **3** and **4**

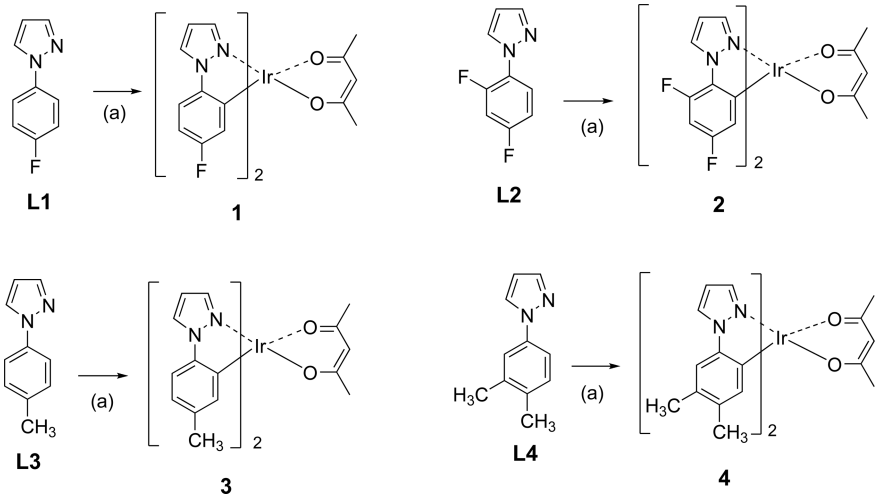

Scheme 1. Structures and synthetic routes of the iridium complexes. (a) i, $IrCl_3 \cdot H_2O$/2-ethoxyethanol/H_2O; ii, 2,4-pentadione/Na_2CO_3/2-ethoxyethanol.

Table 1. Optical properties of complexes **1-4**

Compound	$Ir(ppz)_2acac$	1	2	3	4
UV (nm)[a]	251, 370	216, 270	250, 320	254, 278	237, 255, 370
PL (nm)[b]	509	491	473	510	511
HOMO (eV)[c]	−5.21	−4.89	−4.85	−5.06	−5.04
LUMO (eV)	−1.93	−1.24	−1.25	−1.60	−1.50
E_T	2.44	2.52	2.62	2.43	2.42

[a]Measured in CH_2Cl_2 (1×10^{-5} M at 278 K). [b]Measured in 2-Me THF (1×10^{-5} M at 77 K). [c]The HOMO energy levels were estimated from cyclic voltammetry measurements.

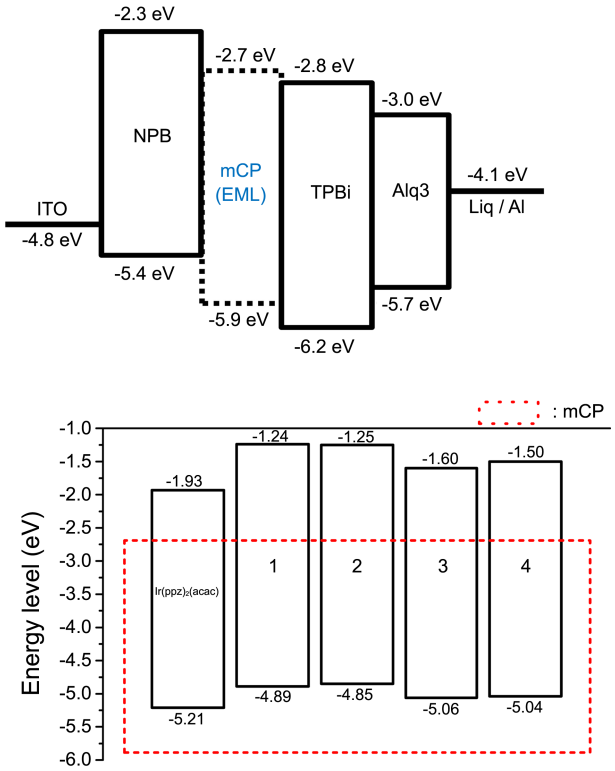

Figure 1. Energy-level diagram of the materials used in devices **A-E**.

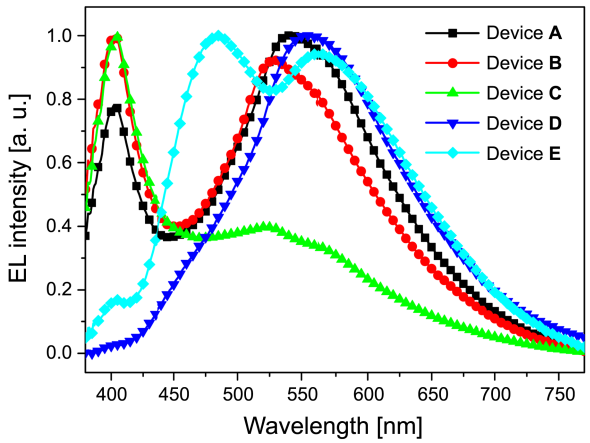

Figure 2. EL spectra of devices **A-E**.

with methyl replaced at the 4-position and 3,4-positions of phenyl ring, revealed 1 nm and 2 nm bathochromic shifts in the PL spectra, respectively. Those shifts in PL spectra imply that introducing functional groups to the phenyl positions affects the triplet energy level. The color tuning would be then possible by such structural modification in the ligands.

The HOMO/LUMO energy levels for the iridium complexes **1-4** were estimated from cyclic voltammetry measurements to −4.89/−1.24, −4.85/−1.25, −5.06/−1.60, and −5.04/−1.50 eV, respectively. These results indicate that the HOMO/LUMO energy levels are very sensitive to the structural features of the ligands.

To explore the EL properties of these complexes **1-4**, multilayered OLED devices were fabricated by employing 8% iridium complexes **1-4** as dopant within mCP host in the emitting layer (devices **B-E**, respectively). For comparison, we also fabricated the device **A** using $Ir(ppz)_2acac$ as dopant at the same doping concentration. The EL results are summarized in Table 2.

Figure 1 shows the device structure and the HOMO/LUMO energy levels of the materials. The NPB was introduced as hole-transporting layer (HTL) to enhance the hole-injection and transporting. The Alq_3 is to function as electron-transporting layer (ETL) while TPBi is to serve as hole-blocking layer.

Figure 2 shows the EL spectra of devices **A-E**. All devices showed the white EL emissions. The corresponding CIE coordinates of devices **A-E** were (0.29, 0.33), (0.29, 0.34), (0.28, 0.32), (0.35, 0.40) and (0.30, 0.34) at 15 V, respectively. Among the devices, device **E** using iridium complex **4** as single emitter showed the most efficient white emission. The EL spectra of device **E** exhibited double emission at 485 nm and 563 nm, which may be originated from iridium complex **4** itself and its excimer, respectively. Consequently, the combination of these two complementary lights may have provided the good white emission. The other devices **A-D** showed the similar behaviors to device E, while the separation of two emission peaks with blue and orange colors are not quite distinct.

To investigate the origin of white emission from devices **A-E**, the PL study of iridium complexes **1-4** in solid film and in diluted CH_2Cl_2 solution were conducted. As shown in Figure 3, the PL spectra of iridium complexes **1-4** in diluted solution showed the blue emissions with the maximum emission peaks of 390-401 nm. However, compared to the PL spectra in diluted solution, the PL spectra in solid film were red-shifted with much broad spectral shapes, which is similar to the EL spectra of devices **A-E**. Particularly, the PL spectrum of iridium complex **4** in solid film showed the double emission at 485 nm and 563 nm, which is similar to

Table 2. The EL characteristics of the devices **A-E**

Device	Dopant	EL (nm)	L[a] (cd/m^2)	LE[b/c] (cd/A)	PE[b/c] (lm/W)	EQE[b/c] (%)	CIE (*x*,*y*)[d]
A	$Ir(ppz)_2acac$	403, 540	175	2.20/0.42	0.99/0.09	0.81/0.24	(0.29, 0.33)
B	1	403,531	160.7	1.15/0.34	0.48/0.08	0.43/0.19	(0.29, 0.34)
C	2	403,523	229.1	0.63/0.43	0.30/0.10	0.38/0.28	(0.28, 0.32)
D	3	481, 555	100.6	1.52/0.33	0.71/0.07	0.59/0.15	(0.35, 0.40)
E	4	485,563	203.2	0.81/0.42	0.33/0.09	0.38/0.22	(0.30, 0.34)

[a]Maximum luminance. [b]Maximum values. [c]At 20 mA/cm^2. [d]CIE values are measured at 15 V.

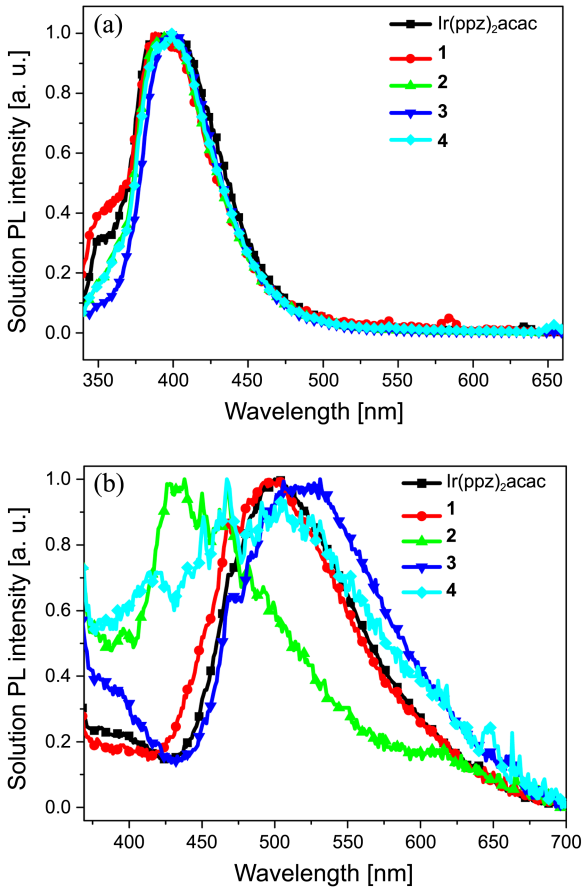

Figure 3. PL spectra of iridium complexes **1-4** (a) in diluted CH_2Cl_2 solution and (b) in solid film.

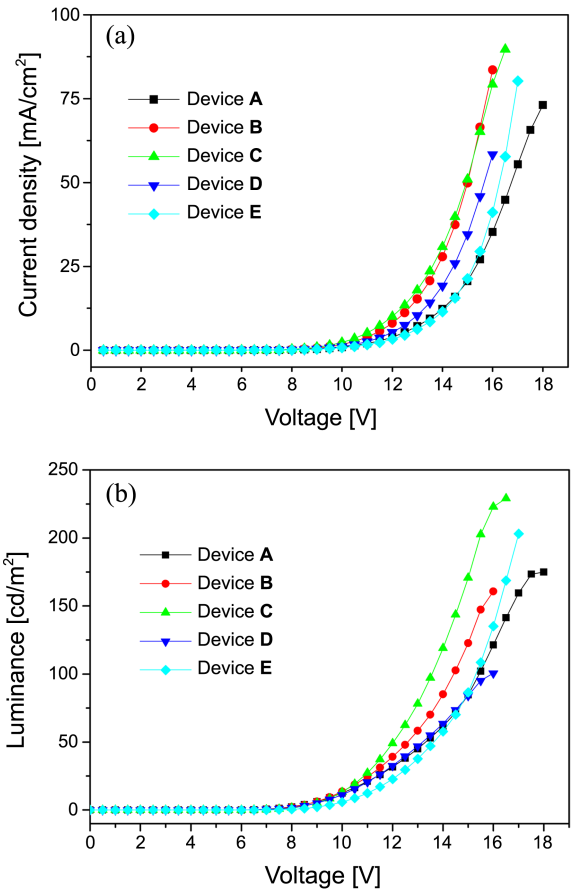

Figure 4. (a) Current density-voltage and (b) luminance-voltage characteristics of devices **A-E**.

the EL spectrum of device **E**. This observation indicates that the white emission of device **E** must be originated from the combined emissions of iridium complex **4** itself and its excimer, respectively. Also, the white emission of other devices **A-D** would be originated from the combined emissions of iridium complexes and their excimers in the corresponding devices.

Figure 4 shows current density-voltage and luminance-voltage characteristics of devices **A-E**. The corresponding current densities of devices **A-E** at 8 V were 0.12, 0.18, 0.25, 0.13 and 0.06 mA/cm^2, respectively. All the devices **A-E** exhibited the low current density at 8 V. Interestingly, the HOMO energy levels of the iridium complexes **1-4** are placed over 0.2 eV higher than that of NPB in HTL layer. The hole trapping process, from NPB into the iridium complexes in the emitting layer, would be efficient in all devices **A-E**. Consequently, these effective hole trapping process would have reduced the current density.

Figure 5 shows power efficiency, the luminous efficiency, and external quantum efficiency versus current density characteristics of devices **A-E**. The corresponding maximum external quantum efficiencies of devices **A-E** were 0.81, 0.43, 0.38, 0.59 and 0.38%, respectively. These low EL efficiencies of devices **A-E** might be explained by the observations that the main emission of devices **A-E** is originated from the corresponding excimers of iridium complexes.

Generally, the emission from the corresponding excimer are less effective than that from emitter-itself, as shown in the concentration quenching phenomena.[12,13] Therefore, devices **A-E** exhibited the reduced EL efficiencies due to aggregation-induced quenching. Interestingly, the EL performances of devices **A-E** are sensitive to the substituents in phenylpyrazole ligands of iridium complexes. Presumably, the degree of excimer formation would depend on the structures of phenylpyrazole ligands of iridium complexes, and thus the structural changes in phenylpyrazole ligands would affect the EL efficiencies of devices **A-E**. For example, compared to device **D**, device **E** showed the improved EL efficiencies. Iridium complex **4** in device **E** has two methyl groups in ligand, while iridium complex **3** in device **D** has only one methyl group. Two methyl groups of iridium complex **4** prevent self-aggregation and thus reduce the degree of excimer formation of iridium complex **4**, in comparison with iridium complex **3**. Thus the bulky substituents of ligands in iridium complexes could lead to the improved EL efficiencies of devices using them. This concept was supported by the EL spectra of devices **D** and **E**. As shown in Figure 2, the EL spectrum of device **E** has much stronger emission peak around 500 nm than that of device **D**, which is originated from iridium complexes **3** and **4**, not their

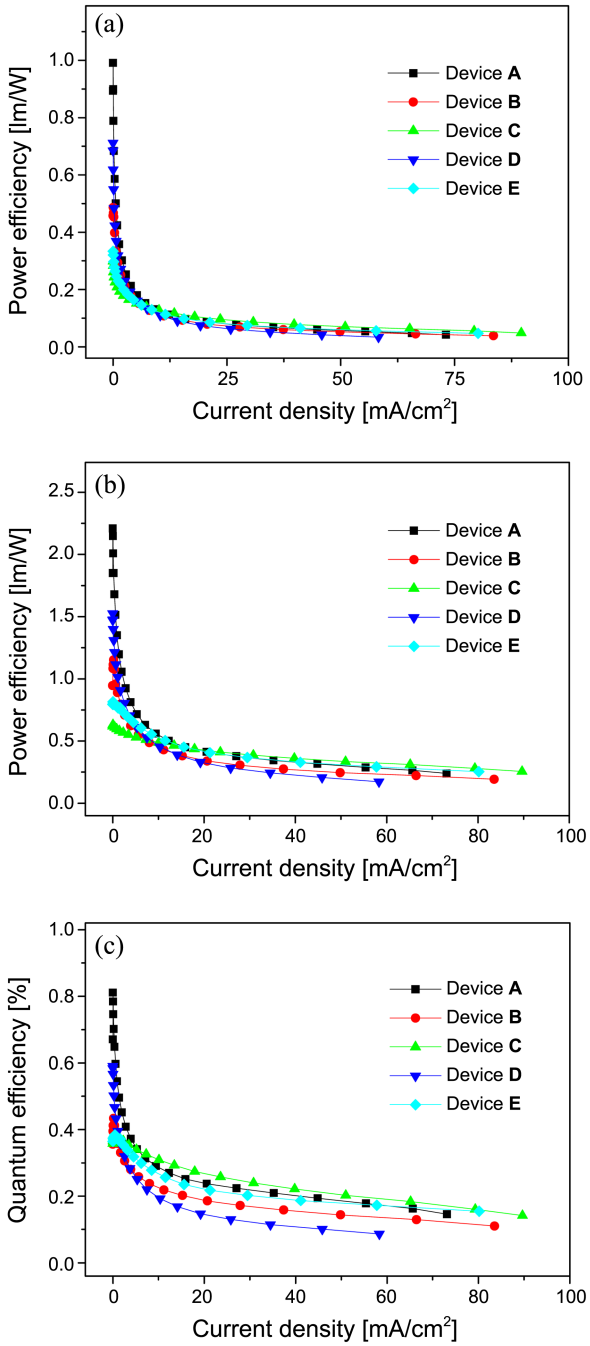

Figure 5. (a) Power efficiency, (b) luminous efficiency, and (c) external quantum efficiency versus current density of devices **A-E**.

corresponding excimers. This suggest that the excimer formation of iridium complex **3** in device **D** is more effective than that of iridium complex **4** in device **E**.

Conclusions

In conclusion, phosphorescent iridium complexes based on 1-phenylpyrazole ligands with fluorine and methyl substitution (**1-4**) for OLEDs were synthesized. All devices using iridium complexes **1-4** as single emitter showed white emission. To enhance the EL efficiencies using these types of iridium complexes as single emitter, a key issue would be the structural modification of ligands to facilitate the excimer formation without loss of emission efficiency from excimers. In this regard, materials with aggregation-induced emission properties[14,15] would contribute to the development of the efficient WOLEDs using single emitter.

Acknowledgments. This paper was supported by Samsung Research Fund, Sungkyunkwan University, 2012.

References and Notes

1. Baldo, M. A.; O'Brien, D. F.; You, Y.; Shoustikov, A.; Siblry, S.; Thompson, M. E.; Forest, S. R. *Nature* **1998**, *395*, 151.
2. Lee, K. H.; Seo, J. H.; Kim, Y. K.; Yoon, S. S. *J. Nanosci. Nanotechnol*. **2009**, *9*, 7099.
3. Lee, K. H.; Kim, J. H.; Seo, J. H.; Kim, Y. K.; Yoon, S. S. *J. Nanosci. Nanotechnol*. **2010**, *10*, 3193.
4. Lee, K. H.; Kang, H. J.; Kim, H. M.; Seo, J. H.; Kim, Y. K.; Yoon, S. S. *J. Nanosci. Nanotechnol.* **2010**, *11*, 1499.
5. Lee, K. H.; Kim, S. O.; Seo, J. H.; Kim, Y. K.; Yoon, S. S. *J. Nanosci. Nanotechnol.* **2011**, *11*, 4471.
6. Kim, J. H.; Nam, E. J.; Hong, S. Y.; Kim, B. O.; Kim, S. M.; Yoon, S. S.; Suh, J. H.; Ha, Y. K.; Kim, Y. K. *Mater. Sci. & Eng. C* **2004**, *24*, 167.
7. Wang, L.; Wong, W.-Y.; Lin, M.-F.; Wong, W.-K.; Cheah, K.-W.; Tam, H.-L.; Chen, C. H. *J. Mater. Chem.* **2008**, *18*, 4529.
8. Williams, E. L.; Haavisto, K.; Li, J.; Jabbour, G. E. *Adv. Mater.* **2007**, *19*, 197.
9. Li, X.; Liu, Y.; Luo, J.; Ahang, Z.; Shi, D.; Chen, Q.; Wang, Y.; He, J.; Li, J.; Lei, G.; Zhu, W. *Dalton Trans*. **2012**, *41*, 2972.
10. He, L.; Duan, L.; Qiao, J.; Dong, G.; Wang, L.; Qiu, Y. *Chem. Mater.* **2010**, *22*, 3535.
11. Lee, H.W.; Chan, A. S. C.; Kwong, F. Y. *Tetrahedron Letters* **2009**, *50*, 5868.
12. Grushin, V. V.; Herron, N.; LeCloux, D. D.; Marshall, W. J.; Petrov, V. A.; Wang, Y. *Chem. Comm*. **2001**, *16*, 1494.
13. Lee, K. H.; Seo, J. H.; Kim, Y. K.; Yoon, S. S. *J. Nanosci. Nanotech.* **2009**, *9*, 7099.
14. Liu, S.; Sun, H.; Ma, Y.; Ye, S.; Liu, X.; Zhou, X.; Mou, X.; Wang, L.; Zhao, Q.; Huang, W. *J. Mater. Chem*. **2012**, *22*, 22167.
15. Zhao, Z.; Lam, J. W. Y.; Tang, B. Z. *J. Mater. Chem*. **2012**, *22*, 23726.